Determination of the tumor tissue optical properties during and after photodynamic therapy using inverse Monte Carlo method and double integrating sphere between 350 and 1000 nm

Norihiro Honda
Katsunori Ishii
Takaya Terada
Takuya Nanjo
Kunio Awazu

SPIE

Determination of the tumor tissue optical properties during and after photodynamic therapy using inverse Monte Carlo method and double integrating sphere between 350 and 1000 nm

Norihiro Honda,[a] Katsunori Ishii,[a] Takaya Terada,[a,b] Takuya Nanjo,[a] and Kunio Awazu[a,b,c,d]
[a]Osaka University, Medical Beam Physics Laboratory, Graduate School of Engineering, 2-1-A14 Yamadaoka, Suita, Osaka, 565-0871, Japan
[b]Development of System and Technology for Advanced Measurement and Analysis, Japan Science and Technology Agency, 5-5 Sanbancho, Chiyoda, Tokyo, 102-0075, Japan
[c]University of Fukui, Research Institute of Nuclear Engineering, 3-9-1 Bunkyo, Fukui, 910-8507, Japan
[d]Kyoto University, Institute for Chemical Research, Gokasho, Uji, Kyoto, 611-0011, Japan

Abstract. Photodynamic therapy (PDT) efficacy depends on the amount of light distribution within the tissue. However, conventional PDT does not consider the laser irradiation dose during PDT. The optical properties of biological tissues (absorption coefficient μ_a, reduced scattering coefficient μ_s', anisotropy factor g, refractive index, etc.) help us to recognize light propagation through the tissue. The goal of this paper is to acquire the knowledge of the light propagation within tissue during and after PDT with the optical property of PDT-performed mouse tumor tissue. The optical properties of mouse tumor tissues were evaluated using a double integrating sphere setup and the algorithm based on the inverse Monte Carlo method in the wavelength range from 350 to 1000 nm. During PDT, the μ_a and μ_s' were not changed after 1 and 5 min of irradiation. After PDT, the μ_s' in the wavelength range from 600 to 1000 nm increased with the passage of time. For seven days after PDT, the μ_s' increased by 1.7 to 2.0 times, which results in the optical penetration depth decreased by 1.4 to 1.8 times. To ensure an effective procedure, the adjustment of laser parameters for the decreasing penetration depth is recommended for the re-irradiation of PDT. © 2011 Society of Photo-Optical Instrumentation Engineers (SPIE). [DOI: 10.1117/1.3581111]

Keywords: optical property; tumor tissue; photodynamic therapy; inverse Monte Carlo technique; double integrating sphere.

Paper 10559PRR received Oct. 13, 2010; revised manuscript received Mar. 30, 2011; accepted for publication Apr. 1, 2011; published online May 19, 2011.

1 Introduction

Photodynamic therapy (PDT) uses a photosensitizer or a photoactivated dye in combination with a visible light that produces a reactive oxygen species and destroys both tumor cells and malignant tissue.[1] The PDT efficacy depends on the light excitation energy distribution, photosensitizer concentration, and oxygen transport and consumption during the treatment. However, conventional PDT does not consider the laser irradiation dose during PDT. For the optimization of treatment planning, it is essential to know how light is transported within the tissue. Using knowledge of the optical properties (absorption coefficient μ_a [mm^{-1}] and reduced scattering coefficient μ_s' [mm^{-1}], etc.) of the target tissue, the light distribution and propagation within the tissue can be estimated.[2]

The change of optical properties by laser treatments is particularly interesting. The light propagation within the tissue changes according to the change of optical properties in laser irradiation.[3,4] Recently, the optical properties of various normal and pathologic tissues have been determined at a single wavelength or over a broad wavelength range. However, there is little information about the change of the optical properties of tissues by PDT in the wide wavelength range.[5–8] The light fluence rate in tissue, by determining the optical properties of PDT-treated tissue, in PDT realizes a pre-estimated and safe treatment effect.

The objective of this study is to determine the optical properties of tissues, which are treated by PDT in the wavelength range from 350 to 1000 nm. In this study, the mouse tumor model that inoculated Lewis lung carcinoma (LLC) cells was used to perform PDT-treatment on tumor tissue. The optical properties of tissues were determined by using the double integrating sphere measurement system[9–13] combined with the inverse Monte Carlo method.[11–16] This paper presents the determination of the optical properties of mouse tumor tissues during and after PDT *in vitro*, and the optical penetration depth of the tumor tissue.

2 Material and Methods

2.1 *Animals Model and Sample Preparation*

Nineteen syngeneic male C57BL/6 mice at six weeks of age were used. The LLC cells were maintained at 37°C and 5% CO_2 in Dulbecco's Modified Eagle's Medium (Sigma-Aldrich Inc., USA) containing 10% fetal calf serum (BioWest Inc., France), 100 units/mL penicillin, and 0.1 mg/mL streptomycin (Nacalai Tesque Inc., Japan). Cells were prepared at 1×10^7 cells/mL for injection. All animals received subcutaneous bolus injections of 0.1 mL of cell suspension in the lower dorsal region using a

Table 1 Experimental conditions of PDT.

Photosensitizer	Talaporfin sodium (Laserphyrin®, MEIJI SEIKA KAISHA, Japan)
Injected dose	5 [mg/kg]
Laser	UM1000 Dental_665 (JENOPTIK unique-mode GmbH, Germany)
Wavelength	664 [nm] (C. W.)
Average power density	100 [mW/cm^2]
Irradiation condition ①	6,30 [J/cm^2] (1,5 min)
Irradiation condition ②	100 [J/cm^2] (16 min 40 s)

23-gauge needle. Each tumor was grown for seven days. Tumor diameter was reached about 11.5 mm on average. For optical property measurement of tissues, the animals were euthanized by an overdose of anesthesia. The tumor tissues were resected using a surgical knife. Then, the skin and the scab of the tissue were removed. The sample was approximately 2 mm in thickness except the sample that was obtained seven days after treatment. The sample thickness of the tissue obtained seven days after treatment was 1 mm due to the removed sample was 1 mm in thickness. Each section was positioned between slide glasses. The optical properties of the tissue were measured with the double integrating sphere setup within 30 min after sacrifice. The animal experimentation was carried out according to the guideline of animal experimentation of Osaka University.

2.2 PDT Treatment

As a photosensitizer, talaporfin sodium (Laserphyrin®, MEIJI SEIKA KAISHA, Japan)[17] was used. 16 tumor-bearing mice were intravenously injected with talaporfin sodium. While the remaining four were control groups without injection. Before injection, talaporfin sodium was reconstituted in the physiological saline and used at a concentration of 5 mg/kg body weight. Talaporfin sodium was injected via the tail vein two hours prior to light exposure. The tumor surface was irradiated superficially through the skin with a laser diode emitting continuous wave laser light at a wavelength of 664 nm (UM1000 Dental_665, JENOPTIK unique-mode GmbH, Germany).[18] The light was collimated with a lens, and the spot diameter was 12.5 mm. The

animals were chosen at random to populate. Table 1 summarizes the treatment conditions. For determination of the tumor tissue optical properties during PDT, the irradiation was performed 1 min to five mice before each measurement of the optical property. And, the light irradiation of 5 min was carried out to five mice. The average power density on the tumor surface was 100 mW/cm^2. For determination of the tissue optical properties after PDT, each tumor of six mice were irradiated with a light dose of 100 J/cm^2. The average power density on the tumor surface was 100 mW/cm^2. During light irradiation, individual animals were restrained un-anesthetized in holders. Then, 1, 2, and 7 days after PDT the tumor tissue was resected and the tissue optical properties were measured.

2.3 Double Integrating Sphere Setup

A double integrating sphere system was designed for the measurement of optical properties of biological tissues. This is also a convenient tool since it simultaneously measures diffuse reflectance (R_d) and total transmittance (T_t). Using an integrating sphere as both a diffuse illumination source and a detector provides a technically simple measurement apparatus. The experimental setup is presented in Fig. 1.

Balanced deuterium tungsten halogen source (DH-2000-BAL, Ocean Optics, USA) combined with high-powered halogen light source (HL-2000-HP, Ocean Optics, USA) were employed as a light source. Specimens were placed between two integrating spheres (FOIS-1, Ocean Optics, USA). The integrating sphere was 38.1 mm inner diameter. The inside
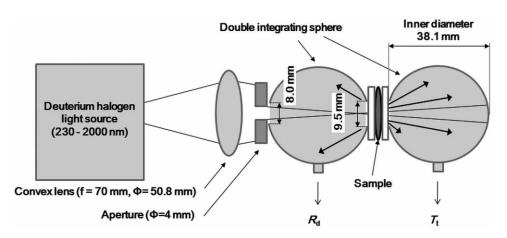

Fig. 1 Schematic of double integrating sphere setup.

surface of the sphere was coated with diffusely reflective material, Spectralon™. The entrance port size of the reflectance sphere was 8.0 mm in diameter and the sample port of both spheres was 9.5 mm in diameter. The beam-illuminated area was 3 mm in diameter on the sample. The incident light was diffusely reflected from the sample surface and the light was diffusely transmitted during the sample. Then, the reflected and transmission light were multiply scattered in spheres and recorded by spectrophotometer (Maya2000 Pro, Ocean Optics, USA) as R_d and T_t, respectively. From these experimental data, the set of optical properties were calculated using the inverse Monte Carlo technique.

2.4 Inverse Monte Carlo Method

The inverse Monte Carlo technique was employed to calculate the optical properties of samples from measured values of R_d and T_t. Calculation of the tissue optical properties was performed at each wavelength point. The algorithm consists of following steps: a. To calculate the optical parameters (R_d and T_t) with Monte Carlo simulations, which was developed by Wang et al.,[2] an initial set of optical properties had been estimated. b. The Monte Carlo simulation was performed on this initial set of data. c. A simulated set of the optical parameters was compared to the actual measurements. If agreement between calculated and measured data was within a defined error limit ($<0.5\%$), the set of optical parameters was accepted for the sample. d. This procedure was repeated with a new set of optical properties until the error threshold was achieved. With this iterative process, the set of optical properties that yields the closest match to the measured values of reflectance and transmittance are taken as optical properties of the tissue. This method allows one to determine the μ_a and μ_s of a tissue from the measured values. Then, the μ'_s was calculated by

$$\mu'_s = \mu_s (1 - g), \quad (1)$$

where g is the anisotropy factor of scattering. In these calculations, g was fixed at 0.9, since this value is typical for many tissues.[19] It is known that the volume-averaged refractive index of most biological tissue falls within 1.34 to 1.62 (Ref. 20) and the refractive index of the lung tissue is 1.38.[21] Therefore, the refractive index of the sample is assumed to be 1.38 in this study.

2.5 Histological Study

Tumors were harvested after PDT and fixed in 8% buffered formalin. The tumors were then embedded in paraffin and stained by hematoxylin and eosin.

2.6 Statistical Analysis

A student's t-test was used to evaluate the significance of the difference between obtained optical properties of tumor tissues. The differences between optical coefficients of control and PDT-treated tissues were considered to be statistically significant when the calculated probability valued (p value) was equal or less than 0.05. P value ≤ 0.05 means that the probability that the two data sets are different is $\geq 95\%$. This level of significance is considered acceptable for the biological samples.
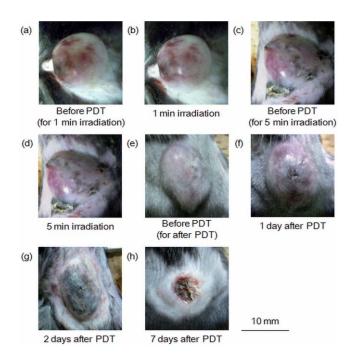

Fig. 2 Photograph of tumor tissues during and after PDT. (a) Gross lesion of tissue before PDT. (b) Tumor tissue after irradiation of 100 mW/cm² for 1 min. (c) Gross lesion of untreated tissue. (d) PDT-treated tissue after completion of irradiation of 100 mW/cm² for 5 min. (e) Tumor tissue before PDT. (f) One day after PDT. Laser irradiation was performed with 100 mW/cm² for 1000 s. (g) Two days after PDT. Tumor was irradiated with 100 mW/cm² for 1000 s. (h) Seven days after PDT. Tumor was irradiated with 100 mW/cm² for 1000 s.

3 Results

3.1 Macroscopic Observations of Photodynamic Therapy Effect

The tumor tissues after 1 and 5 min of irradiation did not show significant changes as shown in Figs. 2(b) and 2(d). However, the PDT-treated tumors showed changes 1, 2, and 7 days after PDT as shown in Figs. 2(f)–2(h). After PDT, a tumor showed a dusky black discoloration.

3.2 Tumor Tissue Optical Properties during Photodynamic Therapy

Optical properties were calculated from the experimental measurements of R_d and T_t of 1 and 5 min irradiated tumor tissues for the determination of the optical property of the tumor tissue during PDT. The R_d and T_t spectra of the tumor tissues are shown in Figs. 3(a) and 3(b), respectively. The μ_a and μ'_s spectra of tumor tissues were shown in Figs. 4(a) and 4(b), respectively. There were several peaks in the μ_a spectra as shown in Fig. 4(a). For tumor tissues before PDT, the peaks were at 439 and 553 nm with mean μ_a values of 1.18 and 0.77 mm^{-1}, respectively. These peaks corresponded to the absorption of the hemoglobin.[22] Scattering, depicted in Fig. 4(b), was greater at shorter wavelength with a peak value of about 1.52 mm^{-1} at the wavelength of 350 nm and smoothly declined over the visible range to a level of about 0.41 mm^{-1} at the wavelength of 1000 nm. During PDT, the μ_a and μ'_s spectra were not changed.
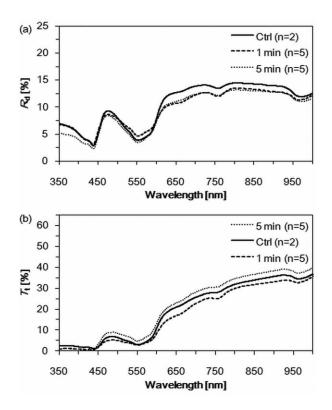
Fig. 3 Diffuse reflectance R_d and transmittance T_t spectra of tumor tissues during PDT. (a) R_d spectra of tumor tissues performed 1 and 5 min irradiation. (b) T_t spectra of the tumor tissues.
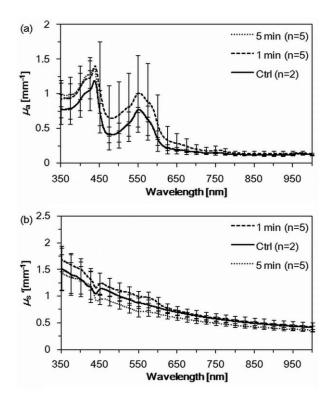
3.3 Tumor Tissue Optical Properties after Photodynamic Therapy

The μ_a and μ_s' spectra of the tumor tissues 1, 2, and 7 days after PDT are shown in Figs. 5(a) and 5(b), respectively. A considerable difference of the mouse tumor tissue optical properties, before and after PDT, was observed. Table 2 summarizes optical properties changes observed in PDT-treated tumor tissues compared with before-treatment tissues in a specific region for PDT-treatment from 600 to 700 nm for the individual wavelengths, such as 632, 664, and 690 nm. After PDT, the values of μ_s' increased with the passage of time as shown in Fig. 5(b).

4 Discussion

4.1 Histological Analysis

It seems clear that a significant increase of μ_s' should be a result of substantial structural changes. As shown in Fig. 6, corresponding changes of mouse tumor tissue structures after PDT were revealed by a histological evaluation of the tumor samples and were compared to sections from non-PDT treated tissue. A histological analysis has shown that PDT causes the blood vessel disruption and leak of erythrocytes [Fig. 6(e)]. Our histological findings confirm the results obtained by Nelson et al.[23] for mouse tumor tissues. It has been shown that specific phenomena, such as microvascular disruption, occur after the completion of PDT. Furthermore, a leak of erythrocytes is caused by vascular damage. A mouse's red blood cell size is about 6 μm in diameter.[24] Blood is a scattering system that consists of scattering particles, such as red blood cells, their aggregates, and the surrounding media (i.e., plasma). The refractive index mismatching between red

Fig. 4 Absorption coefficient μ_a spectra and reduced scattering coefficient μ_s' spectra of tumor tissues during PDT. (a) μ_a spectra of tumor tissues performed 1 and 5 min irradiation. (b) μ_s' spectra of the tumor tissues.
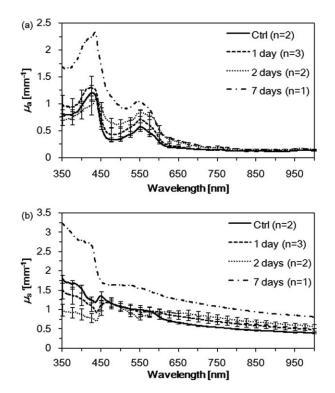

Fig. 5 Absorption coefficient μ_a spectra and reduced scattering coefficient μ_s' spectra of tumor tissues during PDT. (a) μ_a spectra of tumor tissues 1, 2, and 7 days after PDT. (b) μ_s' spectra of the tumor tissues.
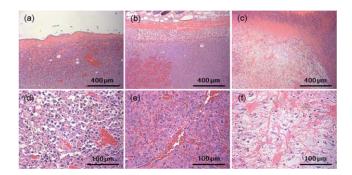
Fig. 6 H&E staining of tumor tissues. (a) and (d) show the Lewis lung carcinoma tissue before PDT. Tumor microvessels are shown. (b) and (e) show the tumor tissues 1 day after PDT. The blood vessel damage and leak of erythrocyte are shown after PDT. (c) and (f) show the PDT treated tumor tissue seven days after PDT. Decrease of tumor cells has been observed. The PDT treated tissue has shown fibrosis.

blood cells cytoplasm and blood plasma is the major source of light scattering in blood.[25] The scattering properties of blood are dependent on RBC volume.[11] As a result, the concentration of chromophores and scattering inhomogeneities increases and tissues become optically denser, which likely leads to a significant increase of μ_s' in the spectral range from 600 to 1000 nm. Seven days after PDT, the PDT-treated tissues showed the decrease of tumor cells and fibrosis as shown in Fig. 6(f). This pathological change has been observed in the clinical treatment[26] and μ_s' of the tissue increased as shown in Fig. 5(b). Saidi et al. found that the large collagen fibers of the dermis were primarily responsible for the light scattering in the skin.[27] They indicated that scattering of normally incident light by a single fiber, as predicted by the Mie theory, was dependent on the wavelength of the indices of refraction of the fibers and of the

surrounding medium. Perhaps, the collagen fibers shown in the PDT-treated tissue played a role of the scatter in the tissue. Then, the μ_s' of the treated tissue measured seven days after treatment increased.

4.2 Penetration Depth of Light within Tumor Tissues during Photodynamic Therapy

The penetration depth of light into a biological tissue is an important parameter for the correct determination of the irradiation dose in the PDT of various diseases. The estimation of the light penetration depth was performed with Eq. (2) (Ref. 28)

$$\sqrt{1/3\mu_a(\mu_a + \mu_s')}. \qquad (2)$$

The optical penetration depth of tumor tissues during PDT was calculated with the calculated optical properties presented in Fig. 4 and the results are presented in Fig. 7(a). The optical penetration depth of the tumor tissues after PDT was calculated with the optical properties presented in Fig. 5 and the result is presented in Fig. 7(b). Table 3 summarizes the optical penetration depth changes observed in PDT-treated tumor tissues compared with before-treatment tissues in a specific region for PDT-treatment from 600 to 700 nm for the individual wavelengths, such as 632, 664, and 690 nm. Comparison of the tumor tissue optical properties before PDT obtained in this study and those presented by Bargo et al.[29] shows an agreement between them. The μ_a and μ_s' spectra of the sample are qualitatively similar to the reported spectra in the spectral range from 600 to 900 nm. Literature values[29] for *in vivo* optical properties of

Table 2 Tumor tissue optical properties during and after PDT.

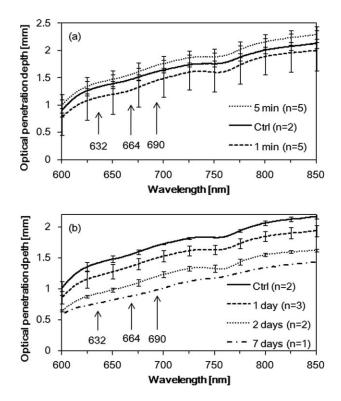| Wavelength [nm]	Post-treatment [days]	μ_a [mm^{-1}] Mean $\pm$ S. D.	μ_s' [mm^{-1}] Mean $\pm$ S. D.
	Before PDT	0.19 ± 0.01	0.69 ± 0.03
632	1	0.22 ± 0.04	0.85 ± 0.07
	2	0.32 ± 0.04	0.92 ± 0.05
	7	0.35	1.30
	Before PDT	0.17 ± 0.01	0.64 ± 0.02
664	1	0.19 ± 0.02	0.80 ± 0.07
	2	0.26 ± 0.04	0.90 ± 0.08
	7	0.29	1.24
	Before PDT	0.16 ± 0.01	0.60 ± 0.01
690	1	0.16 ± 0.01	0.76 ± 0.07
	2	0.22 ± 0.03	0.87 ± 0.09
	7	0.25	1.18

Fig. 7 Optical penetration depth of PDT-treated tumor tissues. (a) Optical penetration depth of tumor tissues during PDT. (b) Optical penetration depth of tumor tissues after PDT.

Table 3 Optical penetration depth of tumor tissues during and after PDT.

Wavelength [nm]	Post-treatment [days]	Penetration depth [mm] Mean ± S. D.
	Before PDT	1.40 ± 0.06
632	1	1.20 ± 0.14
	2	0.92 ± 0.02
	7	0.76
	Before PDT	1.54 ± 0.05
664	1	1.35 ± 0.10
	2	1.05 ± 0.05
	7	0.87
	Before PDT	1.69 ± 0.02
690	1	1.49 ± 0.09
	2	1.19 ± 0.05
	7	0.97

human lung tumor tissues at the wavelength of 630 nm have μ_a ranging from 0.097 to 0.488 mm^{-1} and μ'_s ranging from 0.63 to 1.15 mm^{-1}, which are in agreement with the results obtained in this study.

During PDT, the penetration depth of light was not changed. Recently, the optical properties of *in vivo* human prostate during motexafin lutetium-medicated photodynamic therapy has been presented by Zhu et al. for the wavelength 732 nm.[8] For the wavelength, the effective attenuation coefficient varied after PDT, although the magnitude of the change was generally much smaller. The inverse of the effective attenuation coefficient gives us an estimation of the penetration depth. These results are compatible with our results on the optical penetration depth obtained in this study. Swartling et al. researched the interstitial PDT with online feedback to deliver a tailored light fluence dose, exceeding a predefined threshold dose, to the whole prostate gland and adapt the dose plan in cases where the optical attenuation changes during the therapy.[30] They have reported that the optical properties of the gland tissue did not markedly vary during the treatment with Foscan® in clinical study. But, Thompson et al. reported that light transmission decreased in nodular basal cell carcinomas during 5-amino levulinic acid mediated PDT.[31] They discuss that the light transmission changes are in fact due to the tissue oxygenation and changes in blood volume. Therefore, a system for interactively controlling the treatment to achieve the optimal therapy adapted for each case is needed in light dosimetry during PDT.

After PDT, the penetration depth decreased with the passage of time as shown in Table 3. Compared to the tissue obtained before the treatment, the optical penetration depth of the tissue seven days after PDT decreased by 1.4 to 1.8 times. In general, if the cancer was not cured after the first PDT-treatment, a second

treatment was carried out in PDT.[32] In this study, we found the fact that the optical properties of PDT-treated tumor were changed. As a result, the light penetration depth of the mouse tumor tissues decreased after PDT. For precisely conducting the re-irradiation of PDT, the irradiation dose might be determined based on the optical properties of the PDT-treated tissues. The PDT-treated tissue optical properties will continue to be studied until a complete recovery is obtained and will be presented in future work.

It is difficult to accurately estimate the experimental error in a study of this type in which many independent measurements are conducted. Experimental contributions to the error included the inaccuracy of the spectrometer, which we estimate to be <1% of the corresponding 100% value. This error becomes more prominent as the measured values of R_d and T_t become smaller, such as in the wavelength between 350 nm to 600 nm. Furthermore, there is a significant biological variability between the samples. For example, if the blood of the samples varied, this would be particularly noticeable in the wavelength range between 350 to 600 nm. This may have introduced an error in the μ'_s spectra as shown in Figs. 4(b) and 5(b).

5 Conclusion

The change of the optical properties of mouse tumor tissues by PDT in the wavelength range from 350 to 1000 nm were measured with the double integrating sphere system and the inverse Monte Carlo technique. No significant change could be detected during PDT. The optical property of the tumor tissue dramatically changed after PDT. Especially, the μ'_s increased after PDT. After PDT-treatment, resulting in the change of mouse tumor tissue optical property, the light penetration depth into the tumor tissue decreased with the passage of time. To ensure the effective treatment procedure, an adjustment of the laser parameter in view of the decreasing penetration depth is recommended for the re-irradiation PDT. These tissue parameters become available for more models to predict optical distributions in tissues. The optical property obtained *in vitro* using the combination of double integrating sphere measurements and an inverse Monte Carlo technique are clearly useful for *in vivo* applications.

References

1. A. P. Castano, T. N. Demidova, and M. R. Hamblin, "Mechanisms in photodynamic therapy: part three-photosensitizer pharmacokinetics, biodistribution, tumor localization and modes of tumor destruction," *Photodiagnosis Photodyn. Ther.* **2**(2), 91–106 (2005).
2. L.-H. Wang, S. L. Jacques, and L. Q. Zheng, "MCML – Monte Carlo modeling of photon transport in multi-layered tissues," *Comput. Methods Programs Biomed.* **47**(2), 131–146 (1995).
3. A. N. Yaroslavsky, P. C. Schulze, I. V. Yaroslavsky, R. Schober, F. Ulrich, and H.-J. Schwarzmaier, "Optical properties of selected native and coagulated human brain tissues in vitro in the visible and near infrared spectral range," *Phys. Med. Biol.* **47**(12), 2059–2073 (2002).

4. J.-P. Ritz, A. Roggan, C. Isbert, G. Muller, H. J. Buhr, and C.-T. Germer, "Optical properties of native and coagulated porcine liver tissue between 400 and 2400 nm," *Lasers Surg. Med.* **29**(3), 205–212 (2001).

5. R. van Hillegersberg, J. W. Pickering, M. Aalders, and J. F. Beek, "Optical properties of rat liver and tumor at 633 nm and 1064 nm: photofrin enhances scattering," *Lasers Surg. Med.* **13**(1), 31–39 (1993).

6. A. M. K. Nilsson, R. Berg, and S. Andersson-Engels, "Measurements of the optical properties of tissue in conjunction with photodynamic therapy," *Appl. Opt.* **34**(21), 4609–4619 (1995).

7. H.-J. Wei, D. Xing, J.-J. Lu, H.-M. Gu, G.-Y. Wu, and Y. Jin, "Determination of optical properties of normal and adenomatous human colon tissues *in vitro* using integrating sphere techniques," *World J. Gastroenterol.* **11**(16), 2413–2419 (2005).

8. T. C. Zhu, A. Dimofte, J. C. Finlay, D. Stripp, T. Busch, J. Miles, R. Whittington, S. B. Malkowicz, Z. Tochner, E. Glatstein, and S. M. Hahn, "Determination of the distribution of light, optical properties, drug concentration, and tissue oxygenation in-vivo in human prostate during motexafin lutetium-mediated photodynamic therapy," *J. Photochem. Photobiol., B* **79**(3), 231–241 (2005).

9. J. W. Pickering, S. A. Prahl, N. van Wieringen, J. F. Beek, H. J. C. M. Sterenborg, and M. J. C. van Gemert, "Double-integrating-sphere system for measuring the optical properties of tissue," *Appl. Opt.* **32**(4), 399–410 (1993).

10. G. de Vries, J. F. Beek, G. W. Lucassen, and M. J. C. van Gemert, "The effect of light losses in double integrating spheres on optical properties estimation," *IEEE J. Sel. Top. Quantum Electron.* **5**, 944–947 (1999).

11. A. Roggan, M. Friebel, K. Dörschel, A. Hahn, and G. Müller, "Optical properties of circulating human blood in the wavelength range 400–2500 nm," *J. Biomed. Opt.* **4**(1), 36–46 (1999).

12. T. L. Troy and S. N. Thennadil, "Optical properties of human skin in the near infrared wavelength range of 1000 to 2200 nm," *J. Biomed. Opt.* **6**(2), 167–176 (2001).

13. H.-J. Wei, D. Xing, G.-Y. Wu, H.-M. Gu, J.-J. Lu, Y. Jin, and X.-Y. Li, "Differences in optical properties between healthy and pathological human colon tissues using a Ti:sapphire laser: an *in vitro* study using the Monte Carlo inversion technique," *J. Biomed. Opt.* **10**(4), 044022 (2005).

14. M. Meinke, G. Müller, J. Helfmann, and M. Friebel, "Optical properties of platelets and blood plasma and their influence on the optical behavior of whole blood in the visible to near infrared wavelength range," *J. Biomed. Opt.* **12**(1), 014024 (2007).

15. M. Friebel, A. Roggan, G. Müller, and M. Meinke, "Determination of optical properties of human blood in the spectral range 250 to 1100 nm using Monte Carlo simulations with hematocrit-dependent effective scattering phase functions," *J. Biomed. Opt.* **11**(3), 034021 (2006).

16. E. Salomatina, B. Jiang, J. Novak, and A. N. Yaroslavsky, "Optical properties of normal and cancerous human skin in the visible and near-infrared spectral range," *J. Biomed. Opt.* **11**(6), 064026 (2006).

17. Meiji Seika Kaisha, Ltd., http://www.meiji.co.jp/.

18. Jenoptik unique-mode GmbH, http://www.photonicsonline.com/storefronts/uniquemode.html/.

19. V. V. Tuchin, "Optical properties of tissues with strong (multiple) scattering," Chapter 1 in *Tissue Optics*, pp. 3–17, SPIE Press, Bellingham, WA (2007).

20. L.-H. V. Wang and H. Wu, "Scattering and its biological origins," Chapter 1 in *Biomedical Optics: Principles and Imaging*, pp. 1–16, Wiley, New York (2007).

21. F. P. Bolin, L. E. Preuss, R. C. Taylor, and R. J. Ference, "Refractive index of some mammalian tissues using a fiber optic cladding method," *Appl. Opt.* **28**(12), 2297–2303 (1989).

22. Oregon Medical Laser Center at Providence St. Vincent Medical Center: http://omlc.ogi.edu/spectra/hemoglobin/index.html.

23. J. S. Nelson, L.-H. Liaw, A. Orenstein, W. G. Roberts, and M. W. Berns, "Mechanism of tumor destruction following photodynamic therapy with hematoporphyrin derivative, chlorin, and phthalocyanine," *J. Natl. Cancer Inst.* **80**(20), 1599–1605 (1988).

24. H. Joshima, M. Kashima, and O. Matsuoka, "Diminished osmotic fragility of mouse erythrocytes following intravenous injection of polymeric plutonium," *J. Radiat. Res. (Tokyo)* **25**(4), 290–295 (1984).

25. X. Xu, R. K. Wang, J. B. Elder, and V. V. Tuchin, "Effect of dextran-induced changes in refractive index and aggregation of optical properties of whole blood," *Phys. Med. Biol.* **48**, 1205–1221 (2003).

26. K. F. M. Fan, C. Hopper, P. M. Speight, G. A. Buonaccorsi, and S. G. Bown, "Photodynamic therapy using mTHPC for malignant disease in the oral cavity," *Int. J. Cancer* **73**(1), 25–32 (1997).

27. I. S. Saidi, S. L. Jacques, and F. K. Tittel, "Mie and Rayleigh modeling of visible-light scattering in neonatal skin," *Appl. Opt.* **34**(31), 7410–7418 (1995).

28. R. Splinter and B. A. Hooper, "Light-tissue interaction variables," Chapter 5 in *An Introduction to Biomedical Optics*, pp. 121–154, Taylor & Francis, London (2007).

29. P. R. Bargo, S. A. Prahl, T. T. Goodell, R. A. Sleven, G. Koval, G. Blair, and S. L. Jacques, "*In vivo* determination of optical properties of normal and tumor tissue with white light reflectance and an empirical light transport model during endoscopy," *J. Biomed. Opt.* **10**(3), 034018 (2005).

30. J. Swartling, J. Axelsson, G. Ahlgren, K. M. Kalkner, S. Nilsson, S. Svanberg, K. Svanberg, and S. Andersson-Engels, "System for interstitial photodynamic therapy with online dosimetry: first clinical experience of prostate cancer," *J. Biomed. Opt.* **15**(5), 058003 (2010).

31. M. S. Thompson, A. Johansson, T. Johansson, S. Andersson-Engels, S. Svanberg, N. Bendsoe, and K. Svanberg, "Clinical system for interstitial photodynamic therapy with combined on-line dosimetry measurements," *Appl. Opt.* **44**(19), 4023–4031 (2005).

32. C. Fritsch, G. Goerz, and T. Ruzicka, "Photodynamic therapy in dermatology," *Arch. Dermatol.* **134**, 207–214 (1998).